



Published in final edited form as:

Nat Struct Mol Biol. 2016 August ; 23(8): 730–737. doi:10.1038/nsmb.3250.

Neddylation requires glycyI-tRNA synthetase to protect activated E2

Zhongying Mo^{1,2}, Qian Zhang^{1,2}, Ze Liu^{1,2}, Janelle Lauer³, Yi Shi^{1,2}, Litao Sun^{1,2}, Patrick R. Griffin³, and Xiang-Lei Yang^{1,2,*}

¹Department of Chemical Physiology, The Scripps Research Institute, La Jolla, CA 92037, USA

²Department of Cell and Molecular Biology, The Scripps Research Institute, La Jolla, CA 92037, USA

³Department of Molecular Therapeutics, The Scripps Research Institute, Jupiter, FL 33458, USA

Abstract

Neddylation is a post-translational modification that controls cell cycle and proliferation by conjugating the ubiquitin-like protein NEDD8 to specific targets. Here we report that glycyI-tRNA synthetase (GlyRS), an essential enzyme for protein synthesis, also plays a critical role in neddylation. In human cells, knockdown of GlyRS, but not a different tRNA synthetase, decreases the global level of neddylation and causes cell cycle abnormality. This function of GlyRS is achieved through direct interactions with multiple components of the neddylation pathway, including NEDD8, E1, and E2 (Ubc12). Using various structural and functional approaches, we show that GlyRS binds to the APPBP1 subunit of E1 to capture and protect the activated E2 (NEDD8-conjugated Ubc12) before it reaches a downstream target. Therefore, GlyRS functions as a chaperone to critically support neddylation. This function is likely to be conserved in all eukaryotic GlyRS, and may contribute to the strong association of GlyRS with cancer progression.

Neddylation—conjugating the ubiquitin-like protein NEDD8 to its target proteins—is an essential biological process in organisms from yeast to mammals to critically regulate cell cycle progression¹⁻⁴. Like ubiquitination, the modification is achieved through a sequential enzymatic cascade involving an activating enzyme (E1), a conjugating enzyme (E2), and a ligase (E3) (Fig. 1a). To date, one E1 (APPBP1-UBA3), two E2 (Ubc12 [also known as Ube2M] and Ube2F), and many E3 ligases have been found for neddylation⁵⁻⁸ (Fig. 1a). Although numerous NEDD8 targets were reported⁹, the biological functions of neddylation so far have been primarily characterized in the context of its main targets—the cullin proteins, key components of the ubiquitin E3 cullin-RING ligase family. Neddylation of

Users may view, print, copy, and download text and data-mine the content in such documents, for the purposes of academic research, subject always to the full Conditions of use:http://www.nature.com/authors/editorial_policies/license.html#terms

*To whom correspondence may be addressed: Tel.: 858-784-8976; Fax: 858-784-7250; xlyang@scripps.edu.

CONTRIBUTIONS

X.-L.Y. and Z.M. designed experiments, analyzed data, and wrote the manuscript. Z.M. performed the molecular cloning, binding analysis, structural docking, bioinformatic analysis, and additional biochemical analysis. Z.M. and Q.Z. carried out protein purification. Z.M. and Z.L. performed the cell cycle analysis. J.L. and P.R.G. performed the hydrogen-deuterium exchange analysis. Y.S. and L.S. contributed to biochemical analysis.

cullin activates the E3 ligases for ubiquitination and promotes the degradation of their downstream targets, including key regulators of cell cycle¹⁰.

The initial interest to find a connection between ubiquitination (or ubiquitin-like modifications) and glycyl-tRNA synthetase (GlyRS) was based on molecular considerations. Ubiquitin and most ubiquitin-like modifier proteins, including NEDD8, have a conserved C-terminal glycine that is used to activate, conjugate, and finally attach the modifiers to their targets¹¹. Structurally, the glycine residue is located at the tip of a flexible 'tail' protruding out from the central ubiquitin fold to provide accessibility¹². The well-known function of GlyRS is to catalyze the formation of glycyl-tRNA^{Gly} as a substrate for ribosomal protein synthesis in a two-step reaction¹³: first, GlyRS activates glycine with ATP to generate Gly-AMP; second, the glycyl moiety is transferred from Gly-AMP to the 3' end of tRNA^{Gly}. Interestingly, this first step reaction catalyzed by GlyRS is chemically equivalent to that by an E1 enzyme for activating ubiquitin and ubiquitin-like proteins. Moreover, our previous work indicated that the specific amino acid binding pocket of a tRNA synthetase could be exploited for binding to a cognate amino acid residue on a protein to develop new functions¹⁴.

We set out to test whether human GlyRS can interact with ubiquitin or ubiquitin-like proteins such as NEDD8 and SUMO1 and found that GlyRS specifically binds to NEDD8. Although we did not find an E1-like activity in GlyRS as initially speculated, we did find that GlyRS binds to both E1 and E2 (Ubc12) for neddylation. Moreover, when Ubc12 is conjugated with NEDD8, its affinity for GlyRS is substantially enhanced, suggesting that GlyRS may function to protect activated E2 before it finds the correct downstream targets. Indeed, knockdown of GlyRS, but not of another tRNA synthetase, substantially decreased the level of activated Ubc12 and the level of cullin neddylation in human cells. Consistently, knockdown of GlyRS mimics the effect of MLN4924, a specific inhibitor of E1 for neddylation, and caused cell cycle arrest. Therefore, our study revealed a chaperone-like function of GlyRS to critically support neddylation.

RESULTS

GlyRS specifically binds to NEDD8 and enhances neddylation

Using purified recombinant proteins, we found that human GlyRS can specifically bind to NEDD8, but not ubiquitin or SUMO1 (Fig. 1b). We also tested two other human tRNA synthetases (SerRS and TrpRS) side-by-side and neither of them showed interaction with NEDD8, ubiquitin, or SUMO1 (Fig. 1b). We further verified the GlyRS-NEDD8 interaction in HEK293 cells by co-immunoprecipitation (Fig. 1c). By using truncated recombinant proteins, we mapped the interaction to the catalytic domain of GlyRS (Fig. 1d, e). Hydrogen-deuterium exchange (HDX) analysis confirmed that the catalytic domain was the site for interaction with NEDD8 (Supplementary Fig. 1a).

To test the effect of GlyRS in neddylation, first we ectopically expressed GlyRS in HEK293 cells. Overexpression of GlyRS (but not TrpRS) increased the amount of NEDD8-conjugated Ubc12 (E2 for neddylation), but not the ubiquitin-conjugated UbcH7 (E2 for ubiquitination⁶) or SUMO-conjugated Ubc9 (E2 for sumoylation⁷) (Fig. 1f). Removal of the

metazoan-specific WHEP domain from GlyRS (WHEP) did not substantially affect the activity of GlyRS, while the anticodon-binding domain (ABD) alone had no activity (Fig. 1f), further indicating the involvement of the catalytic domain. Consistently, knockdown of GlyRS expression in HeLa cells led to substantial decrease of NEDD8-conjugated Ubc12 (Ubc12^{N8}) (Fig. 1g), but not the conjugated UbcH7^{Ub} and Ubc9^{Sumo} (Fig. 1h, i). (Similar result was obtained using HEK293 cells (data not shown).) Knockdown of a different tRNA synthetase (SerRS) had no effect on all E2s we tested (Fig. 1g, h, i). Moreover, knockdown of GlyRS, but not SerRS, also substantially decreased the global level of neddylation, including neddylation of cullin proteins (Fig. 1g). We noted that GlyRS knockdown had no effect on E1 neddylation (UBA3^{N8}) or the level of free NEDD8 (Fig. 1g). Also, GlyRS knockdown did not affect Ube2F (Supplementary Fig. 2a), the other E2 for neddylation that is evolutionarily more recent and less used than Ubc12^{N8}. These results suggest that GlyRS is required for neddylation, and that GlyRS is likely to function through promoting or preserving Ubc12^{N8}.

GlyRS preferentially binds and protects Ubc12^{N8}

Ubc12 exists in two forms in the cell, the free form and the conjugated form Ubc12^{N8} made by transferring a NEDD8 molecule from E1 to the catalytic cysteine (Cys111) of Ubc12 (E2) *via* a thioester bond¹⁵. Importantly, once NEDD8 is transferred from E1 to E2, E2^{N8} would be released from E1¹⁶. We speculate that GlyRS may promote the cellular level of Ubc12^{N8} by facilitating the formation of Ubc12^{N8} or by protecting Ubc12^{N8} after it is released from E1. Two separate *in vitro* NEDD8 conjugation assays using either radioactive or fluorescence labeled NEDD8 consistently indicated that GlyRS did not affect the production of Ubc12^{N8} (Supplementary Fig. 3a, b). In contrast, we found that GlyRS substantially enhanced the stability of Ubc12^{N8} *in vitro* (Supplementary Fig. 4), which could explain the activity of GlyRS in promoting the cellular level of Ubc12^{N8}.

We hypothesized that the protection may come from a strong interaction between GlyRS and Ubc12^{N8}. We firstly investigated if GlyRS, in addition to interacting with NEDD8, could also interact with Ubc12. Interestingly, both GST pull-down and HDX analysis confirmed that GlyRS indeed could also bind to Ubc12 and again the catalytic domain of GlyRS is primarily responsible for the interaction (Supplementary Fig. 3c, d). To quantify the binding, we used biolayer interferometry and immobilized GlyRS on a sensor chip to measure its interaction with Ubc12, NEDD8, and Ubc12^{N8}. Remarkably, GlyRS binds to Ubc12^{N8} with a K_d of 4.09 ± 0.30 nM, which is 100-fold and 30-fold stronger than its binding to Ubc12 alone ($K_d = 488 \pm 73$ nM) and to NEDD8 alone ($K_d = 126 \pm 19$ nM), respectively (Fig. 2a). We also analyzed the GlyRS-Ubc12^{N8} interaction reversely by immobilizing Ubc12^{N8} and obtained a similar K_d of 3.21 ± 0.17 nM (Fig. 2b). Consistent with a lack of effect of GlyRS knockdown on the cellular level of Ube2F^{N8} (Supplementary Fig. 2a), the interaction between GlyRS and Ube2F was much weaker, if any, than that between GlyRS and Ubc12 (Supplementary Fig. 2b). We also performed a co-immunoprecipitation experiment using HEK293 cells. Relative to the amount of input, substantially more Ubc12^{N8} than the free Ubc12 was co-immunoprecipitated with GlyRS (Fig. 2c), confirming that GlyRS strongly binds to the NEDD8-conjugated Ubc12 in the cell.

Using the crystal structure of human GlyRS¹⁷ and of Ubc12^{N8} (adapted from its complex with substrate cullin and E3)¹⁸, we generated a model for the GlyRS-Ubc12^{N8} interaction using the Patchdock algorithm (<http://bioinfo3d.cs.tau.ac.il/PatchDock/>)^{19,20}. The top result places Ubc12^{N8} binding to the catalytic domain of GlyRS, with NEDD8 snuggled in between two β -hairpin loops (F84-L93 and I232-M238) (Fig. 2d). (This model is in general consistency with the HDX analysis results (Supplementary Fig. 1a and Fig. 3d).) To validate the model, we created two deletion mutants of the β -hairpin loops (84-93 and 232-238) and found that 84-93 decreased binding of GlyRS to Ubc12^{N8} by 9 fold ($K_d = 27.0 \pm 0.40$ nM) and 232-238 abolished the binding (Fig. 2e, f). In contrast, deletion of an insertion domain unique to GlyRS (Insertion 1)²¹, which shows no involvement in the GlyRS-Ubc12^{N8} interaction according to the model (Fig. 2d), had no effect on the binding ($K_d = 4.32 \pm 0.12$ nM) (Fig. 2g). Consistent with its loss of binding to Ubc12^{N8}, the 232-238 GlyRS was inactive in protecting Ubc12^{N8} from degradation *in vitro* (Supplementary Fig. 4a) and in promoting the level of Ubc12^{N8} in HEK293 cells (Fig. 2h).

GlyRS binds to E1 to facilitate capture of Ubc12^{N8}

Interestingly, we found that GlyRS could also bind to the heterodimeric E1 enzyme for neddylation (APPBP1-UBA3) (Fig. 3a and supplementary Fig. 5a). However, unlike NEDD8 and Ubc12, E1 binds to ABD domain of GlyRS, as revealed by both biolayer interferometry analysis and GST pull-down (Fig. 3a and supplementary Fig. 5a). Furthermore, APPBP1-UBA3 heterodimer and the APPBP1 subunit alone have similar binding affinity for ABD (Fig. 3b), suggesting that APPBP1 subunit of E1 is responsible for the GlyRS interaction. We further validated the APPBP1-GlyRS interaction by co-immunoprecipitation in HEK293 cells (Fig. 3c). Consistently, modeling study using Patchdock placed ABD for interacting with the APPBP1 subunit of the E1 (Supplementary Fig. 5b).

The fact that GlyRS uses different domains to interact with E1 and Ubc12^{N8} suggests that GlyRS may be able to bind to E1 and Ubc12^{N8} simultaneously. As mentioned, once NEDD8 is transferred from E1 to Ubc12, the interaction between them is weakened to release Ubc12^{N8} from the catalytic subunit UBA3 of E1. Perhaps, by binding to the APPBP1 subunit of E1 through the ABD domain, GlyRS is in proximity to capture the released Ubc12^{N8} and provide protection (Fig. 3d).

We designed an experiment to test this concept. We immobilized E1 to detect its interaction with Ubc12^{N8} and GlyRS, separately and simultaneously. As expected, the binding of Ubc12^{N8} to E1 was weak and the disassociation was fast (Fig. 3e). In contrast, the binding of GlyRS to E1 was strong (Fig. 3e). Interestingly, when both Ubc12^{N8} and GlyRS were present, the overall binding was stronger than the sum of the individual bindings (Fig. 3e), suggesting that a ternary complex of E1-GlyRS-Ubc12^{N8} was formed to prevent Ubc12^{N8} from releasing to the solvent.

The ABD of GlyRS was used as a control for this experiment. Although ABD domain alone interacted with the E1 as strongly as the full length GlyRS (Fig. 3 a, b), the absence of the catalytic domain of GlyRS for capturing Ubc12^{N8} would not allow the formation of a

ternary complex. Indeed, we did not detect a synergistic effect between ABD and Ubc12^{N8} for binding to E1 (Fig. 3f).

GlyRS does not interfere with NEDD8 downstream transfer

Because we observed a tight binding between GlyRS and Ubc12^{N8}, it is important to confirm that the binding does not impede Ubc12^{N8} from passing NEDD8 down to its targets such as cullin1. Notably, the protection of Ubc12^{N8} by GlyRS does not seem to require burying the thioester linkage. In our GlyRS-Ubc12^{N8} complex model, the thioester bond between the C-terminal glycine residue Gly76 of NEDD8 and Cys111 of Ubc12 is facing outward rather than buried inside (Fig. 2d) and is fully accessible to the acceptor residue Lys720 of cullin1 (Supplementary Fig. 6a). Using RING-box protein 1 (Rbx1)-cullin1 as the E3-substrate pair, we tested if it can bind to Ubc12^{N8} in the presence of GlyRS. We found that not only Rbx1-cullin1 could bind to Ubc12^{N8} in the presence of GlyRS; the binding seemed to release GlyRS from Ubc12^{N8} (Supplementary Fig. 6b), presumably allowing GlyRS to turnover. Using an *in vitro* neddylation assay, we further demonstrated that the presence of WT GlyRS, but not 232-238 GlyRS that lacks Ubc12^{N8} binding, increased the neddylation of cullin1, presumably by protecting Ubc12^{N8} (Supplementary Fig. 6c).

GlyRS regulates cell cycle progression

Cullin neddylation activates the cullin-RING ubiquitin ligases and facilitates the degradation of their downstream targets, including cell cycle inhibitor p27 (Fig. 4a)²². p27 induces cell cycle arrest by binding to cyclin-CDK (cyclin-dependent kinase) complexes to inhibit their catalytic activity²³. Therefore, degradation of p27 through cullin neddylation promotes cell cycle progression and cell proliferation. Because this is a well-established pathway, we focused on p27 degradation and cell cycle progression to study the biological role of GlyRS in neddylation.

To evaluate p27 degradation in cells, we used cycloheximide (CHX), an inhibitor of translation, to block new protein synthesis. The level of p27 decreased rapidly upon cycloheximide treatment in untreated HeLa cells or cells transfected with empty vectors or plasmids expressing shRNAs against SerRS (shSerRS) (Fig. 4b). (Proteasome inhibitor MG132 was included to confirm the ubiquitin-dependent proteolysis of p27.) However, knock down of GlyRS (shGlyRS) enhanced the stability of p27 (Fig. 4b), as evidenced by both the increased level of p27 prior to the CHX treatment and the extended half-life of p27 during the treatment. Moreover, the stabilization effect on p27 was concurrent with a decreased level of cullin^{N8} (Fig. 4b). To further confirm this effect is related to neddylation, we used a neddylation specific inhibitor MLN4924²⁴ as the positive control. Indeed, MLN4924 treatment abolished cullin neddylation and blocked p27 degradation (Fig. 4a, b). Abnormal accumulation of p27 would lead to cell cycle arrest²⁵. Consistently, compared with the control cells, cells transfected with shGlyRS or treated with MLN4924 showed a substantial decrease in the number of diploid (2N) cells and increase of tetraploid (4N) cells (Fig. 4c), indicating cell cycle arrest.

Active site is not essential for GlyRS to assist neddylation

Although our study was initially intrigued by the chemical similarity between reactions catalyzed by GlyRS and E1, we have not been able to detect an E1-like activity in GlyRS for NEDD8 (data not shown). Moreover, we found that removal of the c-terminal di-glycine motif of NEDD8 had little impact on the GlyRS-NEDD8 interaction (Supplementary Fig. 1b, c). To further clarify whether the active site and the ability to synthesize Gly-AMP are important for GlyRS to enhance neddylation, we tested a GlyRS mutant G526R. The G to R substitution blocks the ATP binding site of GlyRS (Fig. 5a) and completely abolished the aminoacylation activity¹⁷. However, albeit reduced activity, G526R GlyRS was active in promoting the cellular level of Ubc12^{N8} (Fig. 5b) and in restoring p27 degradation and cell cycle progression in the presence of a low dose of the neddylation inhibitor MLN4924 (Fig. 5c, d), suggesting that the active site or the ability to synthesize Gly-AMP may impact but is not essential for the role of GlyRS in neddylation. Interestingly, we found that G526R GlyRS had a decreased (~10-fold) binding to Ubc12^{N8} ($K_d = 39.5 \pm 1.2$ nM) compared with WT GlyRS (Fig. 5e), which could explain the reduced activity of G526R GlyRS in promoting the cellular level of Ubc12^{N8} and in facilitating neddylation.

DISCUSSION

Human GlyRS contains a metazoan-specific WHEP domain, a catalytic domain and an anticodon-binding domain (ABD) (Fig. 1d). Only the later two domains are essential for tRNA aminoacylation¹⁷, and interestingly both are involved to promote neddylation. Our results from biochemical and structural analysis support the model, in which GlyRS, by docking on the APPBP1 subunit of E1 through the ABD domain, is in proximity to capture, by the catalytic domain, the NEDD8-conjugated E2 (Ubc12^{N8}) after it is released from the E1 and before it finds the correct E3 and substrate to transfer the NEDD8 modifier. The confinement provided by the synthetase would protect the conjugated E2 from random hydrolysis and thereby enhance the overall efficiency of neddylation. It is possible that the protection of GlyRS is essential for neddylation. However, the situation that GlyRS is also essential for protein synthesis and that the same domains of GlyRS are used for both activities complicates the evaluation of this possibility.

Neddylation activates cullin proteins as molecular scaffolds to assemble the Cullin-RING (RING box protein) E3 ubiquitin ligase, the largest family of E3 ligases for ubiquitination. In humans, six members of cullin proteins (cullin1, 2, 3, 4A, 4B, and 5) each assembles with one of the two RING box proteins (Rbx1 and Rbx2) to mediate ubiquitination and degradation of thousands of targets to regulate a vast array of biological functions^{26,27}. In the hierarchical cascade of cullin neddylation, selectivity is achieved through the collaboration of RING and E2. Same as for the RINGs, two E2s for NEDD8 were identified, with Ubc12 specifically pairing with Rbx1 to mediate neddylation of cullin1–4, and Ube2F functioning through Rbx2 to control cullin5 neddylation^{8,28}. Interestingly, Ube2F-Rbx2-cullin5 neddylation constitutes a metazoan-specific NEDD8 cascade⁸, whereas Ubc12, Rbx1, and cullin1 are present in all eukaryotes along with NEDD8 and E1. Although GlyRS is ubiquitously and abundantly present in all organisms, eukaryotic GlyRSs are substantially different from most of their bacterial counterparts²⁹. Our observation that GlyRS specifically

binds with Ubc12 but not Ube2F (Supplementary Fig. 2b) suggests that GlyRS is a component of the prototypic cascade of neddylation and that the role of GlyRS to protect the conjugated Ubc12 to facilitate neddylation may have existed from the beginning when the modification first occurred. Further observations that GlyRS interacts with multiple components of the prototypic neddylation pathway and that the metazoan-specific WHEP domain is dispensable for all these interactions (Fig. 1e, Supplementary Fig. 3c, Supplementary Fig. 5a) are consistent with this concept.

Apparently, dysregulation of neddylation can cause abnormality in protein degradation through the ubiquitin-proteasome system and can play a pathological role in various diseases. It has been reported that high levels of NEDD8 are present in ubiquitinated inclusion bodies in neural tissues collected from patients with neurodegenerative disorders such as Alzheimer's disease, Parkinson's disease, and amyotrophic lateral sclerosis^{30,31}. It is interesting to note that dominant mutations in GlyRS have been found to cause a neurodegenerative disorder called Charcot-Marie-Tooth disease Type 2D (CMT2D) in patients^{32,33}. In fact, the G526R mutation we tested is a CMT2D-causing mutation³⁴. Although G526R GlyRS does exhibit reduced activity relative to the WT protein in binding to Ubc12^{N8} (Fig. 5), genetic studies using mouse models have clearly demonstrated that CMT2D is caused by toxic gain-of-function mechanism rather than loss-of-function of either canonical or non-canonical activities of GlyRS³⁵. Moreover, an aberrant interaction made specifically by mutant but not WT GlyRS with neuropilin 1 has been recently identified to account (at least partially) for the selective motor neuron pathology in CMT2D³⁶. Lastly, no pathological aggregation or ubiquitin-positive inclusion was detected in neural tissues from CMT2D mouse models³⁷, further indicating that dysregulation of neddylation is unlikely to be involved in the etiology of CMT2D.

Up-regulation of neddylation is strongly associated with cancer^{9,38,39}. Many targets of neddylation are involved in regulating cancer progression, including regulators of cell cycle (p27⁴⁰ and cyclin E⁴¹), transcription (NRF2⁴², HIF-1 α ⁴³, and pI κ B α ⁴⁴), and DNA replication (CDT-1⁴⁵). In fact, the neddylation pathway has been recognized as an important anticancer target, and the selective NEDD8 E1 inhibitor MLN4924 is currently being tested in several clinical trials for hematological malignancies and solid tumors^{46,47}. As a component of the translation machinery, GlyRS is expected to be associated with cancer progression, which requires robust protein synthesis activity. However, the critical role of GlyRS in neddylation we revealed in this study suggests that GlyRS might be associated with cancer for an additional reason. Remarkably, when we examined aminoacyl-tRNA synthetase expression in previously generated microarray datasets from 3557 breast cancer patients⁴⁸, we found that GlyRS gives the strongest association with cancer mortality among all 20 aminoacyl-tRNA synthetases (Fig. 6a). Following GlyRS to be on the top of the list are ThrRS and LysRS (Fig. 6a). Notably, ThrRS has been reported as an angiogenic, pro-migratory extracellular signaling molecule⁴⁹ and LysRS was found to promote cancer cell migration and metastasis by inhibiting ubiquitin-dependent degradation of laminin receptor^{50,51}.

In conclusion, by using biochemical, structural, and cell-based approaches, we have discovered that GlyRS, in addition to being an essential enzyme for protein synthesis, also

acts as a chaperone to critically assist neddylation, including neddylation of cullin proteins of the ubiquitin-proteasome system (Fig. 6b). Through the dual function, GlyRS supports both general protein production and selective protein degradation, and by which may play a crucial role in maintaining the homeostasis of the eukaryotic proteome.

ONLINE METHODS

Plasmid construction and protein purification

GST-tagged or untagged human APPBP1-UBA3, Ubc12, and NEDD8 proteins were purified as previously reported⁵². GST-APPBP1 was obtained by injecting the purified GST-APPBP1-UBA3 into the Superdex 200 column and collected the fractions that contained only GST-APPBP1. N-terminal His-SUMO-tagged or His-tagged NEDD8 construct was generated by subcloning the pGEX2TK-NEDD8 into a modified pET28a vector and the proteins were purified using a Nickel-NTA column followed by MonoQ ion exchange column. His-NEDD8 GG was generated by site mutagenesis and purified in a similar manner. Recombinant human ubiquitin and SUMO1 proteins (Bostonbiochem) were purchased. His-tagged full-length and WHEP human GlyRS, SerRS, and TrpRS were purified as reported earlier⁵³⁻⁵⁵. The ABD (V541-E685) of GlyRS was cloned, expressed, and purified in a similar way as for the full-length GlyRS (the yield for ABD alone is higher than that for the full-length GlyRS). Tag-free wild type GlyRS, 84-93 (F84-L93 replaced by GGG), 232-238 (I232-M238 replaced by GG), Insertion1 (F147-F224 replaced by GSGSGG) and G526R GlyRS proteins were expressed with a N-terminal His-SUMO-tag, which is subsequently removed by Ulp1 protease. Inserting the GlyRS sequence into a modified pET28a vector generated N-terminal GST-tagged GlyRS and the protein was purified by glutathione sepharose chromatography. GST-Cullin1_{ctd}/Rbx1 was purified by glutathione sepharose chromatography as well¹⁸. Ube2F protein was prepared as described⁵⁶. The purity of proteins was examined by SDS-PAGE to be above 95%.

Affinity pull-down assay

Glutathione sepharose beads (GE Healthcare) were equilibrated with TEE buffer (50mM Tris pH 7.9), 1mM EDTA, and 1mM EGTA). GST-fusion proteins were mixed with 50 μ l of glutathione sepharose beads and incubated for 2 h at 4°C and then washed with TEE buffer twice. Aliquots of the protein-bound beads were then incubated together with different forms of GlyRS for 2 h at 4°C. Finally, the beads were washed 5 times with washing buffer (20 mM Hepes pH 7.9, 150 mM NaCl, 0.5 mM EDTA, 10 % Glycerol, 0.1% Triton X-100, and 1mM DTT) and proteins were eluted with SDS sample buffer and analyzed by immunoblotting. Control experiments were performed with GST-coated beads. His-tag pull-down assay were carried out in a similar manner using purified his-tagged proteins and incubated with Nickel-NTA beads (Qiagen).

Cell culture and shRNA knockdown

HEK293 and HeLa cells were obtained from ATCC without further authentication. Both cells were cultured in DMEM (11995, Gibco) media supplemented with Pen Strep (15140, Gibco) and 10% FBS (FB-12, Omega). Short-hairpin RNA (shRNA) sequences targeting the human GlyRS (5'-GCATGGAGTATCTCACAAAGT-3') or human SerRS (5'-

GGCATAGGGACCCATCATTGA-3') were inserted into the pLentiLox-hH1 plasmid, modified from the pLentiLox 3.7 plasmid to contain a H1 promoter (between Xba I and Xho I sites) to drive shRNA expression. Sequences of GlyRS (full length or truncations, WT or mutants) or TrpRS were inserted into the pcDNA6v5c plasmid for over-expression purpose. Sequence of Ubc12 (C111S) was inserted into the pFLAG-CMV2 plasmid for over-expression purpose. NEDD8 sequence was inserted into the modified pMyc-CMV2 plasmid for over-expression purpose. All transfection was done with Lipofectamine 2000 (Invitrogen) and cells were harvested 48 h after transfection.

Immunoprecipitation

Two μg of anti-V5 (R96-CUS; Invitrogen), anti-GlyRS (D-10; Santa cruz), anti-myc (9E10; Santa cruz) antibodies or mouse IgG (#5415; Cell Signaling) were coupled to 30 μL of protein G-sepharose (Amersham Biosciences) beads and used for immunoprecipitations. Supernatant of HEK293 cells lysates were then added and incubated with the antibodies for 3 h or overnight at 4°C. The G-sepharose beads were then washed four times with 1 mL of cold PBS buffer (pH 7.4). The beads-bound proteins were eluted and denatured with SDS-loading buffer and subjected to SDS-PAGE and Western blotting.

Immunoblotting and antibodies

Cells were washed with PBS and then lysed with either the lysis buffer (#9803; Cell Signaling Technology; 20 mM Tris-HCl, pH 7.5, 150 mM NaCl, 1mM Na₂EDTA, 1 mM EGTA, 1% Triton, 2.5 mM sodium pyrophosphate, 1mM β -glycerophosphate, 1mM Na₃VO₄, 1 $\mu\text{g}/\text{mL}$ leupeptin) or the acidic lysis buffer (50 mM HEPES, pH 6.0, 150 mM NaCl, 0.1% (w/v) SDS) supplemented with protease cocktail (Roche). The acidic lysis buffer was used to preserve the ubiquitin or ubiquitin-like conjugations (e.g., UBA3^{N8}, Ubc12^{N8}, UbcH7^{Ub}, Ubc9^{SUMO}) that are labile in the regular lysis buffer. The supernatant of the lysate was used for Western blotting. The antibodies used in this study include anti-cullin1 (H213; Santa cruz), anti-UBA3 (F-10; Santa cruz), anti-GlyRS (B01P; Abnova or sc-98614; Santa cruz), anti-SerRS (homemade), anti-V5 (R96-CUS; Invitrogen), and anti-Ube2F (pa5-26641; Thermo Fisher). Other antibodies including anti-NEDD8 (#2754), anti-Ubiquitin (#3936), anti-SUMO1 (#4930), anti-Ubc12 (#5641), anti-Ubc9 (#4918), anti-Flag (#2908), anti-UBA1 (#4891), anti-UbcH7 (#3848), anti-UBA2 (#8688), anti-APPBP1 (#14321), anti-p27kip (#3698), and anti- α -Tubulin (#3873) are from Cell Signaling.

Hydrogen-Deuterium exchange mass spectrometry

Solution-phase amide HDX was carried out with a fully automated system as described previously⁵⁷. Briefly, 4 μL of protein was diluted to 20 μL with D₂O-containing buffer and incubated at 4°C for 10, 30, 60, 900, or 3600 s. Samples were diluted to 50 μL with 3M urea, 1% TFA at 1°C to denature the proteins and minimize back-exchange. Samples were then passed across an immobilized pepsin column at 50 $\mu\text{L}/\text{min}$ in 0.1% TFA at 15°C. Resulting peptides were trapped on a C8 cartridge (Hypersil Gold; Thermo Fisher). Peptides were then gradient eluted (4% CH₃CN to 40% CH₃CN, 0.3% formic acid) at 1°C across a 1mm \times 50mm C18 reversed phase HPLC column (Hypersil Gold; Thermo Fisher) and electrosprayed directly into an orbitrap mass spectrometer (either LTQ Orbitrap or Q-Exactive; Thermo Fisher). Data were processed with in-house software⁵⁸ and visualized

with PyMol (Schrödinger, LLC). To measure the difference in exchange rates, we calculated the average percent deuterium uptake for unbound GlyRS protein at all time points. From this value, we subtracted the average percent deuterium uptake for GlyRS protein bound to NEDD8. Negative perturbation values indicate exchange rates are slower for GlyRS bound to NEDD8, which suggests the region is less accessible to amide exchange due to structural alteration or direct contact between GlyRS and NEDD8. GlyRS-Ubc12 interaction was analyzed in a similar way.

In vitro neddylation with γ -³²P-ATP labeled NEDD8

The assay was performed as described by Huang *et. al*⁸. Briefly, 20 μ g NEDD8 proteins were freshly labeled by γ -³²P-ATP using protein kinase A (9U/ μ g) at room temperature for 2 h. Then 5 μ M Ubc12 was charged at RT with γ -³²P-ATP modified NEDD8 in the reaction buffer (50 mM Tris, 50 mM NaCl, 5 mM MgCl₂, pH 7.6) in the presence of 0.3 μ M E1, 5mM ATP, 1 mM DTT, 2mg/mL BSA, 10U/mL pyrophosphatase, 10U/mL creatine kinase, 5mM creatine phosphate with or without 50 μ M GlyRS. The reaction was then quenched at 10min by adding 2 \times SDS loading buffer and the samples were subjected to SDS-PAGE and the gel was visualized by autoradiography.

In vitro neddylation with fluorescein modified NEDD8

The fluorescein modified NEDD8 (Boston biochem, UL-830-050) was used for this assay. Briefly, the reaction was initiated by mixing 0.3 μ M APPBP1-UBA3, 5 μ M Ubc12, 25 μ M NEDD8, 1 mM Mg²⁺-ATP with or without 5 μ M GlyRS in the reaction buffer (50 mM Hepes, 50 mM NaCl, pH 8.0). The mixture was incubated at 37°C and quenched after 30min by adding 2 \times SDS loading buffer. The samples were then prepared and subjected to SDS-PAGE. The gel was then visualized by FluochemM system (Proteinsimple).

Ubc12^{N8} preparation and stability assay

The conjugated Ubc12^{N8} was prepared by mixing 0.2 μ M APPBP1-UBA3, 7 μ M Ubc12 (C111S; the mutant would form a stable ester linkage to NEDD8), 10 μ M His-SUMO-tagged NEDD8 in 50 mM Tris pH 8.0 buffer supplemented with 50 mM NaCl, 1 mM MgCl₂, and 2 mM ATP. The mixture was incubated at 25°C for 16 h. Ubc12^{N8} was then purified by gel filtration chromatography using a Superdex 200 column. The fractions containing only Ubc12^{N8} were concentrated and used for the study. The purity of proteins was examined by SDS-PAGE to be above 95%.

The wild type Ubc12^{N8} conjugation was prepared in a similar manner except at pH 5.5 (NaOAc). Ubc12^{N8} was then purified by gel filtration chromatography using a Superdex 200 column. The fractions containing only Ubc12^{N8} were concentrated and used for the study. The purity of proteins was examined by SDS-PAGE to be above 95%. The stability assay was carried out by incubating 6.9 μ M Ubc12^{N8} with 6.9 μ M GlyRS or 6.9 μ M 232-238 in PBS buffer (with 5 mM DTT) at 37° for indicated times. Samples were then subjected to SDS-PAGE and stained with coomassie blue. Image of the gels were then quantified using ImageJ and the calculated amount of Ubc12^{N8} was plotted against time.

Biolayer interferometry

The dissociation constants (K_d) were obtained with biolayer interferometry by using an Octet QK system (FortéBio). Samples or buffer were dispensed into 96-well plates (Greiner Bio-one) at 200 μ L per well. Operating temperature was maintained at 30 °C. Proteins were diluted into kinetic buffer (PBS with 0.1% BSA and 0.002% Tween-20) and immobilized on either anti-GST or Ni-NTA sensor tips. The other proteins were diluted using the same buffer into a range of different concentrations. Assays with Ubc12^{N8} (Ubc12_{C111S}^{N8-His}) were carried out using the acidic kinetic buffer (50 mM NaOAc pH 5.5, 50 mM NaCl, 0.1% BSA, and 0.002% Tween-20). The raw data were processed by subtraction to reference cells and then aligned with associations (0.2-0.4s). The dissociation constants K_d were obtained by fitting the processed data using the 1:1 model in the Octet analysis software with $R^2 > 0.99$ and labeled as mean \pm S.D.

Molecular modeling

The Ubc12^{N8}-GlyRS interaction is obtained by using the Patchdock^{19,20} server. GlyRS (PDB: 2PME) is assigned as the receptor and Ubc12^{N8} (PDB: 4P5O chain G, H) is assigned as the ligand. Clustering RMSD is set at 4.0. The GlyRS-APPBP1 interaction is modeled using similar settings with APPBP1-UBA3 (PDB: 2NVU chain A&B) assigned as the receptor and GlyRS assigned as the ligand. Molecular visualization and analysis were performed using PyMOL (Schrödinger, LLC). The transient interaction between E1 and Ubc12^{N8} is modeled by aligning the NEDD8 molecule from the above two crystal structures.

In vitro cullin1 neddylation assay

The reaction was initiated by mixing 0.3 μ M APPBP1-UBA3, 5 μ M Ubc12, 25 μ M NEDD8, 2.6 μ M GST-cullin1_{ctd}/Rbx1, 13 μ M WT or 232-238 GlyRS, and 1 mM Mg²⁺-ATP in the reaction buffer (50 mM Hepes, 50 mM NaCl, pH 8.0). The mixture was then incubated at 37°C for 1 h and quenched by adding E1 quench buffer (1 mM EDTA). The samples were then prepared by adding the SDS loading buffer and subjected to SDS-PAGE and Western blot analysis.

Cycloheximide chasing assay

HeLa cells at 80% confluence were transfected using Lipofectamine 2000 with pLentiLox-hH1 vectors containing either a specific sequence targeting GlyRS, SerRS or the vector alone. Forty-eight hours after transfection, medium was replaced with that containing 30 μ g/mL cycloheximide (#2112; Cell signalling) or 20 μ M MG-132 (#508338, Fisher). MLN4924 (I-502; Boston-biochem) samples were prepared by treating the cells with 0.2 μ M MLN4924 for 24 h and then followed by cycloheximide or MG132 treatment. Samples were collected and lysed with acidic lysis buffer and later subjected to SDS-PAGE.

FACS analysis

HeLa cells at 80% confluence were transfected using Lipofectamine 2000 with pLentiLox-hH1 vectors containing either a scramble sequence or a specific sequence targeting GlyRS or SerRS. Forty-eight hours after transfection, cells were treated with medium containing either

0.2 μ M MLN4924 or same amount of DMSO. Twenty-four hours after treatment, cells were washed once with sorting buffer (PBS plus 1% FBS) and collected using 0.05% Trypsin. The mixture was then centrifuged at 500g to collect the cell pellets. Cells were then washed twice with sorting buffer and then suspended and fixed with 70% EtOH at 4°C for 2 h. After fixation, cells were washed twice with sorting buffer and suspended with the propidium iodide (PI) staining solution. Samples were later analyzed by flow cytometry (BD FACS Canto; BD Bioscience). HeLa cells at 80% confluence were transfected using Lipofectamine 2000 with pcDNA6v5c vectors or vectors inserted with either WT GlyRS or G526R GlyRS. Forty-eight hours after transfection, cells were treated with medium containing 0.2 μ M MLN4924. Twenty-four hours after treatment, cells were collected and processed as aforementioned and analyzed by flow cytometry.

Kaplan-Meier curves for human aminoacyl-tRNA synthetases

Kaplan-Meier curves of human aminoacyl-tRNA synthetases were plotted by using an online survival analysis tool (<http://kmplot.com/analysis/index.php?p=service&cancer=breast>)⁴⁸ with a relapse free survival cohort of 3557 breast cancer patients. The samples were divided into two halves of “low-expression (black)” and “high-expression (red)” sets and only JetSet best probe results were used to draw the plots. The follow up time course was set at 17 years to calculate the p value and hazard ratio (HR).

Supplementary Material

Refer to Web version on PubMed Central for supplementary material.

ACKNOWLEDGEMENTS

We thank B. Schulman (St. Jude Children’s Research Hospital) and W. Harper (Harvard medical school) for providing plasmids and advice on the project. We thank P. Schimmel, W. He, H. Zhou, M.H. Nawaz, and other members of The Scripps Laboratories for tRNA Synthetase Research for advice, discussion, reagents, and technical support. This research is supported by US National Institutes of Health grant R01GM088278 (X.-L.Y.).

REFERENCES

1. Kamitani T, Kito K, Nguyen HP, Yeh ET. Characterization of NEDD8, a developmentally down-regulated ubiquitin-like protein. *J Biol Chem.* 1997; 272:28557–62. [PubMed: 9353319]
2. Osaka F, et al. Covalent modifier NEDD8 is essential for SCF ubiquitin-ligase in fission yeast. *EMBO J.* 2000; 19:3475–84. [PubMed: 10880460]
3. Tateishi K, Omata M, Tanaka K, Chiba T. The NEDD8 system is essential for cell cycle progression and morphogenetic pathway in mice. *J Cell Biol.* 2001; 155:571–9. [PubMed: 11696557]
4. Kerscher O, Felberbaum R, Hochstrasser M. Modification of proteins by ubiquitin and ubiquitin-like proteins. *Annu Rev Cell Dev Biol.* 2006; 22:159–80. [PubMed: 16753028]
5. Liakopoulos D, Doenges G, Matuschewski K, Jentsch S. A novel protein modification pathway related to the ubiquitin system. *EMBO J.* 1998; 17:2208–14. [PubMed: 9545234]
6. Osaka F, et al. A new NEDD8-ligating system for cullin-4A. *Genes Dev.* 1998; 12:2263–8. [PubMed: 9694792]
7. Furukawa M, Zhang Y, McCarville J, Ohta T, Xiong Y. The CUL1 C-terminal sequence and ROC1 are required for efficient nuclear accumulation, NEDD8 modification, and ubiquitin ligase activity of CUL1. *Mol Cell Biol.* 2000; 20:8185–97. [PubMed: 11027288]
8. Huang DT, et al. E2-RING expansion of the NEDD8 cascade confers specificity to cullin modification. *Mol Cell.* 2009; 33:483–95. [PubMed: 19250909]

9. Enchev RI, Schulman BA, Peter M. Protein neddylation: beyond cullin-RING ligases. *Nat Rev Mol Cell Biol.* 2015; 16:30–44. [PubMed: 25531226]
10. Soucy TA, Dick LR, Smith PG, Milhollen MA, Brownell JE. The NEDD8 Conjugation Pathway and Its Relevance in Cancer Biology and Therapy. *Genes Cancer.* 2010; 1:708–16. [PubMed: 21779466]
11. Welchman RL, Gordon C, Mayer RJ. Ubiquitin and ubiquitin-like proteins as multifunctional signals. *Nat Rev Mol Cell Biol.* 2005; 6:599–609. [PubMed: 16064136]
12. Vijay-Kumar S, Bugg CE, Cook WJ. Structure of ubiquitin refined at 1.8 Å resolution. *J Mol Biol.* 1987; 194:531–44. [PubMed: 3041007]
13. Bublitz C. The properties of a glycyl-soluble-RNA synthetase from chick embryo. *Biochim Biophys Acta.* 1966; 113:158–66. [PubMed: 4287345]
14. Zhou Q, et al. Orthogonal use of a human tRNA synthetase active site to achieve multifunctionality. *Nat Struct Mol Biol.* 2010; 17:57–61. [PubMed: 20010843]
15. Huang DT, et al. A unique E1-E2 interaction required for optimal conjugation of the ubiquitin-like protein NEDD8. *Nat Struct Mol Biol.* 2004; 11:927–35. [PubMed: 15361859]
16. Eletr ZM, Huang DT, Duda DM, Schulman BA, Kuhlman B. E2 conjugating enzymes must disengage from their E1 enzymes before E3-dependent ubiquitin and ubiquitin-like transfer. *Nature Structural & Molecular Biology.* 2005; 12:933–934.
17. Xie W, Nangle LA, Zhang W, Schimmel P, Yang XL. Long-range structural effects of a Charcot-Marie-Tooth disease-causing mutation in human glycyl-tRNA synthetase. *Proc Natl Acad Sci U S A.* 2007; 104:9976–81. [PubMed: 17545306]
18. Scott DC, et al. Structure of a RING E3 trapped in action reveals ligation mechanism for the ubiquitin-like protein NEDD8. *Cell.* 2014; 157:1671–84. [PubMed: 24949976]
19. Duhovny D, Nussinov R, Wolfson HJ. Efficient unbound docking of rigid molecules. *Algorithms in Bioinformatics, Proceedings.* 2002; 2452:185–200.
20. Schneidman-Duhovny D, Inbar Y, Nussinov R, Wolfson HJ. PatchDock and SymmDock: servers for rigid and symmetric docking. *Nucleic Acids Res.* 2005; 33:W363–7. [PubMed: 15980490]
21. Guo RT, Chong YE, Guo M, Yang XL. Crystal structures and biochemical analyses suggest a unique mechanism and role for human glycyl-tRNA synthetase in Ap4A homeostasis. *J Biol Chem.* 2009; 284:28968–76. [PubMed: 19710017]
22. Pagano M, et al. Role of the ubiquitin-proteasome pathway in regulating abundance of the cyclin-dependent kinase inhibitor p27. *Science.* 1995; 269:682–5. [PubMed: 7624798]
23. Toyoshima H, Hunter T. p27, a novel inhibitor of G1 cyclin-Cdk protein kinase activity, is related to p21. *Cell.* 1994; 78:67–74. [PubMed: 8033213]
24. Soucy TA, et al. An inhibitor of NEDD8-activating enzyme as a new approach to treat cancer. *Nature.* 2009; 458:732–6. [PubMed: 19360080]
25. Hengst L, Reed SI. Translational control of p27Kip1 accumulation during the cell cycle. *Science.* 1996; 271:1861–4. [PubMed: 8596954]
26. Petroski MD, Deshaies RJ. Function and regulation of cullin-RING ubiquitin ligases. *Nat Rev Mol Cell Biol.* 2005; 6:9–20. [PubMed: 15688063]
27. Cardozo T, Pagano M. The SCF ubiquitin ligase: insights into a molecular machine. *Nat Rev Mol Cell Biol.* 2004; 5:739–51. [PubMed: 15340381]
28. Stanley DJ, et al. Inhibition of a NEDD8 Cascade Restores Restriction of HIV by APOBEC3G. *PLoS Pathog.* 2012; 8:e1003085. [PubMed: 23300442]
29. Mazauric MH, et al. Glycyl-tRNA synthetase from *Thermus thermophilus* - Wide structure divergence with other prokaryotic glycyl-tRNA synthetases and functional inter-relation with prokaryotic and eukaryotic glycylation systems. *European Journal of Biochemistry.* 1998; 251:744–757. [PubMed: 9490048]
30. Dil Kuazi A, et al. NEDD8 protein is involved in ubiquitinated inclusion bodies. *J Pathol.* 2003; 199:259–66. [PubMed: 12533840]
31. Mori F, et al. Accumulation of NEDD8 in neuronal and glial inclusions of neurodegenerative disorders. *Neuropathol Appl Neurobiol.* 2005; 31:53–61. [PubMed: 15634231]

32. Antonellis A, et al. Glycyl tRNA synthetase mutations in Charcot-Marie-Tooth disease type 2D and distal spinal muscular atrophy type V. *American Journal of Human Genetics*. 2003; 72:1293–1299. [PubMed: 12690580]
33. Yao P, Fox PL. Aminoacyl-tRNA synthetases in medicine and disease. *Embo Molecular Medicine*. 2013; 5:332–343. [PubMed: 23427196]
34. Dubourg O, et al. The G526R glycyl-tRNA synthetase gene mutation in distal hereditary motor neuropathy type V. *Neurology*. 2006; 66:1721–6. [PubMed: 16769947]
35. Motley WW, et al. Charcot-Marie-Tooth-linked mutant GARS is toxic to peripheral neurons independent of wild-type GARS levels. *PLoS Genet*. 2011; 7:e1002399. [PubMed: 22144914]
36. He W, et al. CMT2D neuropathy is linked to the neomorphic binding activity of glycyl-tRNA synthetase. *Nature*. 2015; 526:710–4. [PubMed: 26503042]
37. Stum M, et al. An assessment of mechanisms underlying peripheral axonal degeneration caused by aminoacyl-tRNA synthetase mutations. *Mol Cell Neurosci*. 2011; 46:432–43. [PubMed: 21115117]
38. Chairatvit K, Ngamkitidechakul C. Control of cell proliferation via elevated NEDD8 conjugation in oral squamous cell carcinoma. *Mol Cell Biochem*. 2007; 306:163–9. [PubMed: 17660949]
39. Salon C, et al. Altered pattern of Cul-1 protein expression and neddylation in human lung tumours: relationships with CAND1 and cyclin E protein levels. *J Pathol*. 2007; 213:303–10. [PubMed: 17823919]
40. Podust VN, et al. A Nedd8 conjugation pathway is essential for proteolytic targeting of p27Kip1 by ubiquitination. *Proc Natl Acad Sci U S A*. 2000; 97:4579–84. [PubMed: 10781063]
41. Nakayama KI, Nakayama K. Ubiquitin ligases: cell-cycle control and cancer. *Nat Rev Cancer*. 2006; 6:369–81. [PubMed: 16633365]
42. Kobayashi A, et al. Oxidative stress sensor Keap1 functions as an adaptor for Cul3-based E3 ligase to regulate proteasomal degradation of Nrf2. *Mol Cell Biol*. 2004; 24:7130–9. [PubMed: 15282312]
43. Kamura T, et al. Activation of HIF1alpha ubiquitination by a reconstituted von Hippel-Lindau (VHL) tumor suppressor complex. *Proc Natl Acad Sci U S A*. 2000; 97:10430–5. [PubMed: 10973499]
44. Winston JT, et al. The SCFbeta-TRCP-ubiquitin ligase complex associates specifically with phosphorylated destruction motifs in IkappaBalpha and beta-catenin and stimulates IkappaBalpha ubiquitination in vitro. *Genes Dev*. 1999; 13:270–83. [PubMed: 9990852]
45. Nishitani H, et al. Two E3 ubiquitin ligases, SCF-Skp2 and DDB1-Cul4, target human Cdt1 for proteolysis. *EMBO J*. 2006; 25:1126–36. [PubMed: 16482215]
46. Sarantopoulos J, et al. Phase I Study of the Investigational NEDD8-Activating Enzyme Inhibitor Pevonedistat (TAK-924/MLN4924) in Patients with Advanced Solid Tumors. *Clin Cancer Res*. 2016; 22:847–57. [PubMed: 26423795]
47. Swords RT, et al. Pevonedistat (MLN4924), a First-in-Class NEDD8-activating enzyme inhibitor, in patients with acute myeloid leukaemia and myelodysplastic syndromes: a phase 1 study. *Br J Haematol*. 2015; 169:534–43. [PubMed: 25733005]
48. Gyorffy B, et al. An online survival analysis tool to rapidly assess the effect of 22,277 genes on breast cancer prognosis using microarray data of 1,809 patients. *Breast Cancer Res Treat*. 2010; 123:725–31. [PubMed: 20020197]
49. Williams TF, Mirando AC, Wilkinson B, Francklyn CS, Lounsbury KM. Secreted Threonyl-tRNA synthetase stimulates endothelial cell migration and angiogenesis. *Sci Rep*. 2013; 3:1317. [PubMed: 23425968]
50. Kim DG, et al. Interaction of two translational components, lysyl-tRNA synthetase and p40/37LRP, in plasma membrane promotes laminin-dependent cell migration. *FASEB J*. 2012; 26:4142–59. [PubMed: 22751010]
51. Kim DG, et al. Chemical inhibition of prometastatic lysyl-tRNA synthetase-laminin receptor interaction. *Nat Chem Biol*. 2014; 10:29–34. [PubMed: 24212136]

REFERENCES FOR ONLINE METHODS

52. Huang DT, Schulman BA. Expression, purification, and characterization of the E1 for human NEDD8, the heterodimeric APPBP1-UBA3 complex. *Methods Enzymol.* 2005; 398:9–20. [PubMed: 16275315]
53. He W, et al. Dispersed disease-causing neomorphic mutations on a single protein promote the same localized conformational opening. *Proc Natl Acad Sci U S A.* 2011; 108:12307–12. [PubMed: 21737751]
54. Sajish M, et al. Trp-tRNA synthetase bridges DNA-PKcs to PARP-1 to link IFN-gamma and p53 signaling. *Nat Chem Biol.* 2012; 8:547–54. [PubMed: 22504299]
55. Xu X, et al. Unique domain appended to vertebrate tRNA synthetase is essential for vascular development. *Nat Commun.* 2012; 3:681. [PubMed: 22353712]
56. Jin J, Li X, Gygi SP, Harper JW. Dual E1 activation systems for ubiquitin differentially regulate E2 enzyme charging. *Nature.* 2007; 447:1135–8. [PubMed: 17597759]
57. Chalmers MJ, et al. Probing protein ligand interactions by automated hydrogen/deuterium exchange mass spectrometry. *Anal Chem.* 2006; 78:1005–14. [PubMed: 16478090]
58. Pascal BD, et al. HDX workbench: software for the analysis of H/D exchange MS data. *J Am Soc Mass Spectrom.* 2012; 23:1512–21. [PubMed: 22692830]

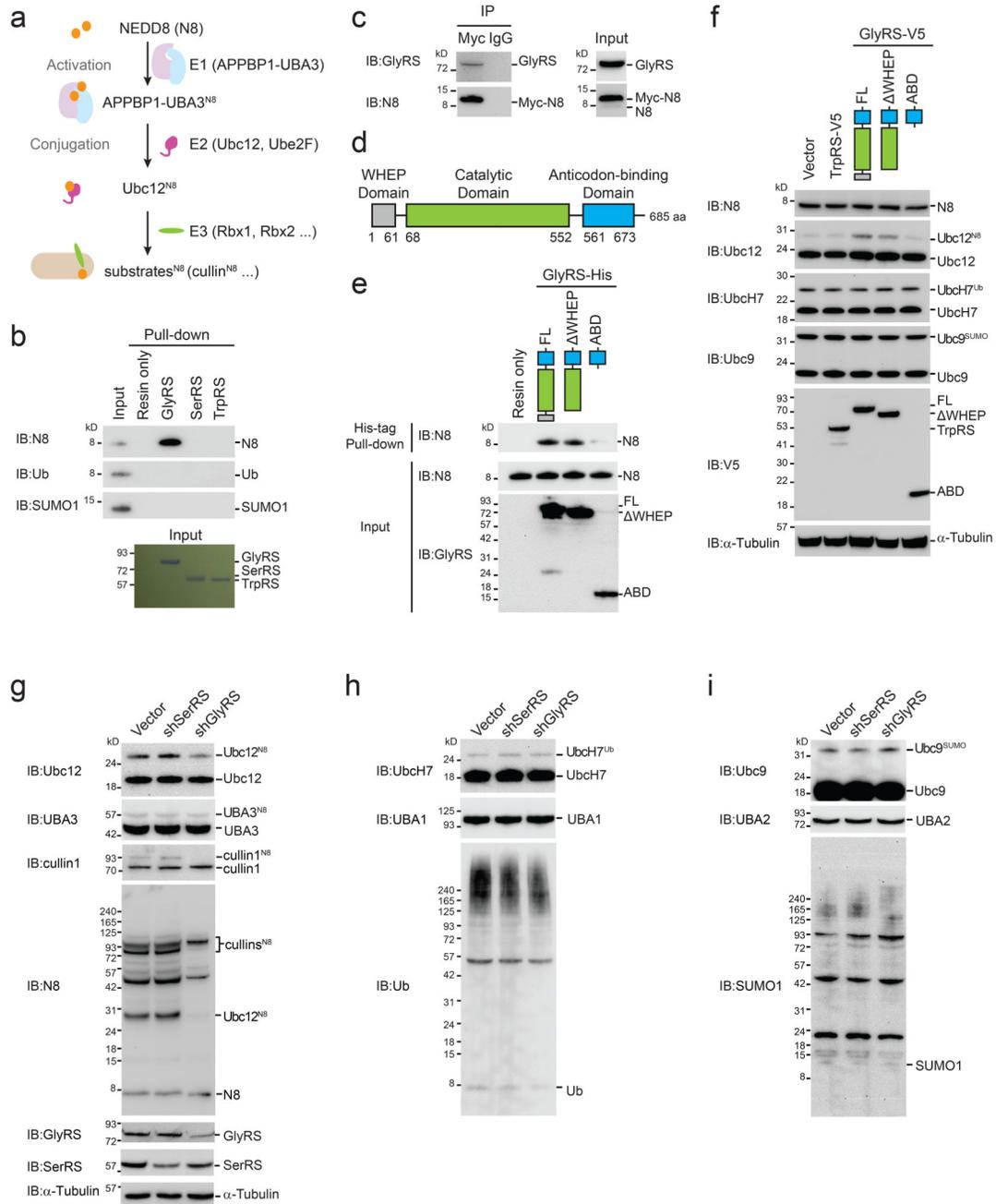


Fig. 1. GlyRS binds to NEDD8 and enhances neddylation

(a) A schematic flowchart of the neddylation pathway. (b) His-tag pull-down assay to test whether the purified recombinant human tRNA synthetases (GlyRS-His₆, SerRS-His₆, and TrpRS-His₆) can interact with purified recombinant NEDD8 (N8), ubiquitin (Ub), and SUMO1 proteins. (c) Co-immunoprecipitation assay to detect GlyRS-NEDD8 binding in HEK293 cells, which were transiently transfected with Myc-NEDD8. (d) Domain composition of human GlyRS. (e) His-tag pull-down assay to map the NEDD8-binding site on GlyRS. (f) Western blot analysis to detect the effect of overexpressing GlyRS or its

fragments on E2 conjugations in HEK293 cells. **(g, h, i)** Western blot analysis of neddylation **(g)**, ubiquitination **(h)** and sumoylation **(i)** cascades components in HeLa cells transfected with plasmids expressing shRNAs against GlyRS (shGlyRS) or SerRS (shSerRS) or a control vector.

Author Manuscript

Author Manuscript

Author Manuscript

Author Manuscript

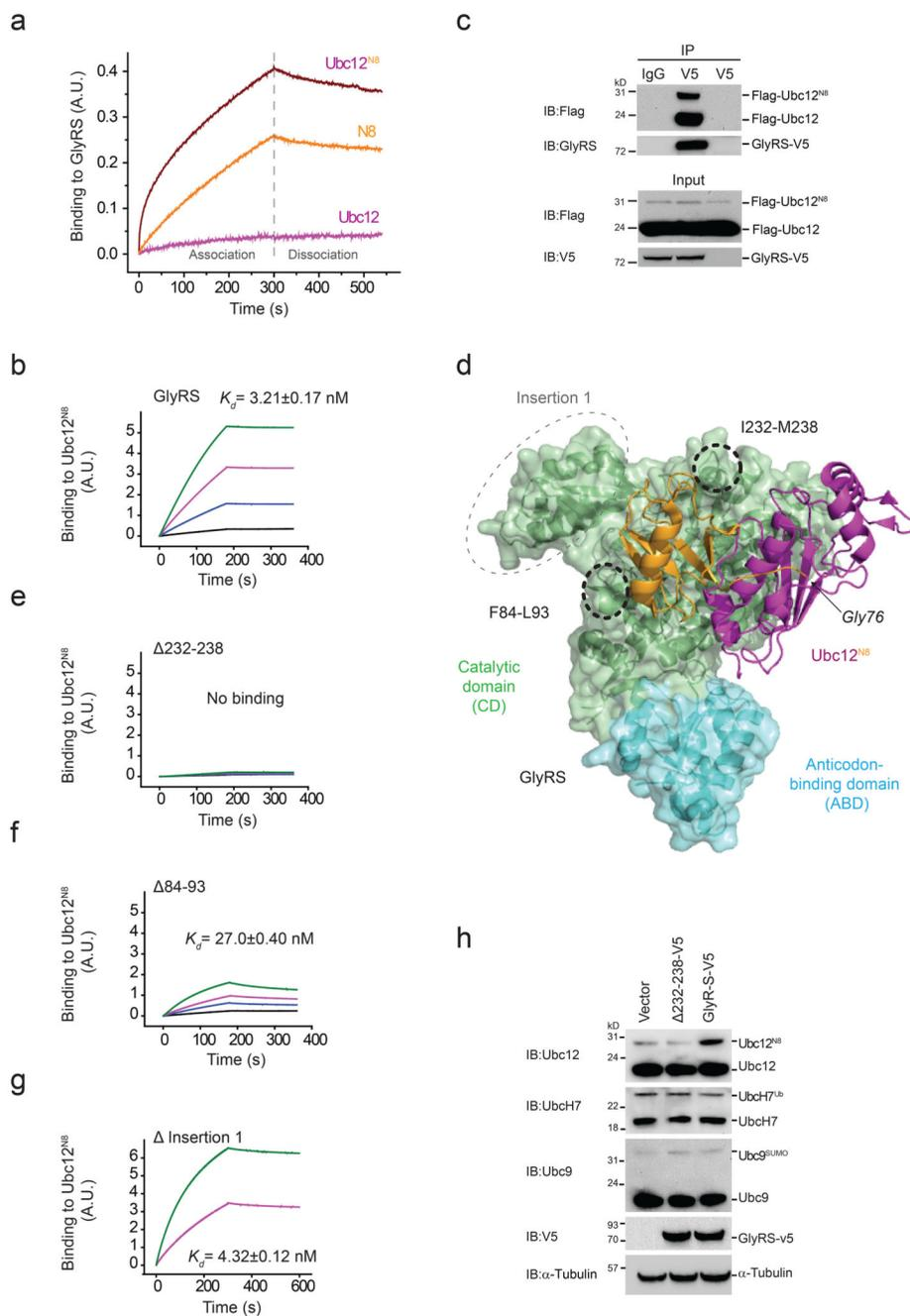


Fig. 2. GlyRS preferentially binds to Ubc12^{N8}

(a) Detection of GlyRS interactions with NEDD8, Ubc12, and Ubc12^{N8} using biolayer interferometry analysis. A.U. indicates Arbitrary Unit. Same concentrations (62.5 nM) of NEDD8, Ubc12, and Ubc12^{N8} were used to bind to the immobilized GST-tagged GlyRS. (b) Biolayer interferometry analysis to detect GlyRS (8-130 nM) binding to immobilized Ubc12^{N8}. N=4, error indicates S.D. (c) Co-immunoprecipitation assay to detect the binding of GlyRS with Ubc12 and with Ubc12^{N8} in HEK293 cells. GlyRS is V5 tagged and Ubc12 is Flag-tagged and C111S mutated to stabilize N8-conjugation. (d) Structural model of the

GlyRS-Ubc12^{N8} complex generated using Patchdock. **(e, f, g)** Biolayer interferometry analysis on 84-93 (8-130 nM) **(e)**, 232-238 (8-130 nM) **(f)**, and Insertion 1 (62.5-125 nM) **(g)** GlyRS for binding to immobilized Ubc12^{N8}. N=3-4, errors indicate S.D. **(h)** Western blot analysis to detect the effect of overexpressing WT versus 232-238 GlyRS on E2 conjugations in HEK293 cells.

Author Manuscript

Author Manuscript

Author Manuscript

Author Manuscript

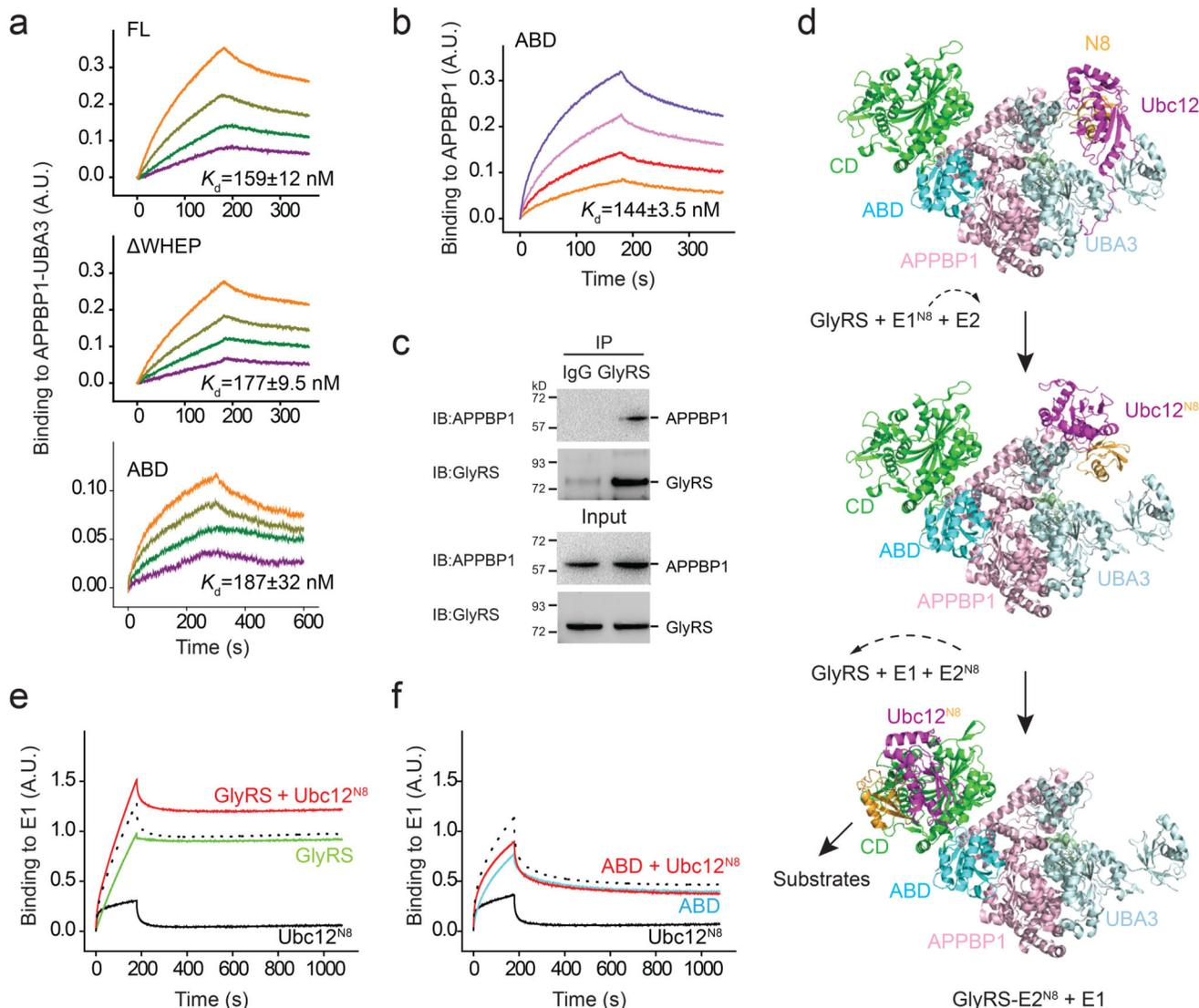


Fig. 3. GlyRS binds to APPBP1 and captures newly released Ubc12^{N8}

(a) Biolayer interferometry analysis comparing full-length, WHEP, and ABD GlyRS (62.5-500 nM) for binding to immobilized E1 (GST-APPBP1-UBA3). N=4, errors indicate S.D. (b) Biolayer interferometry analysis to detect the binding of ABD GlyRS to immobilized GST-APPBP1. N=4, error indicates S.D. (c) Co-immunoprecipitation to detect the GlyRS-APPBP1 interaction in HEK293 cells. (d) Structural model for how GlyRS protects Ubc12^{N8} during the neddylation cascade. (e) Biolayer interferometry analysis to detect the binding of GlyRS (5 μg/mL) or Ubc12^{N8} (5 μg/mL) or both to the immobilized E1 (GST-APPBP1-UBA3). (f) Biolayer interferometry analysis to detect the binding of ABD GlyRS (5 μg/mL) or Ubc12^{N8} (5 μg/mL) or both to the immobilized E1 (GST-APPBP1-UBA3). Black dotted lines indicate the calculated sum of the binding curves for Ubc12^{N8} and for full-length GlyRS (e) or for ABD GlyRS (f) to E1, respectively.

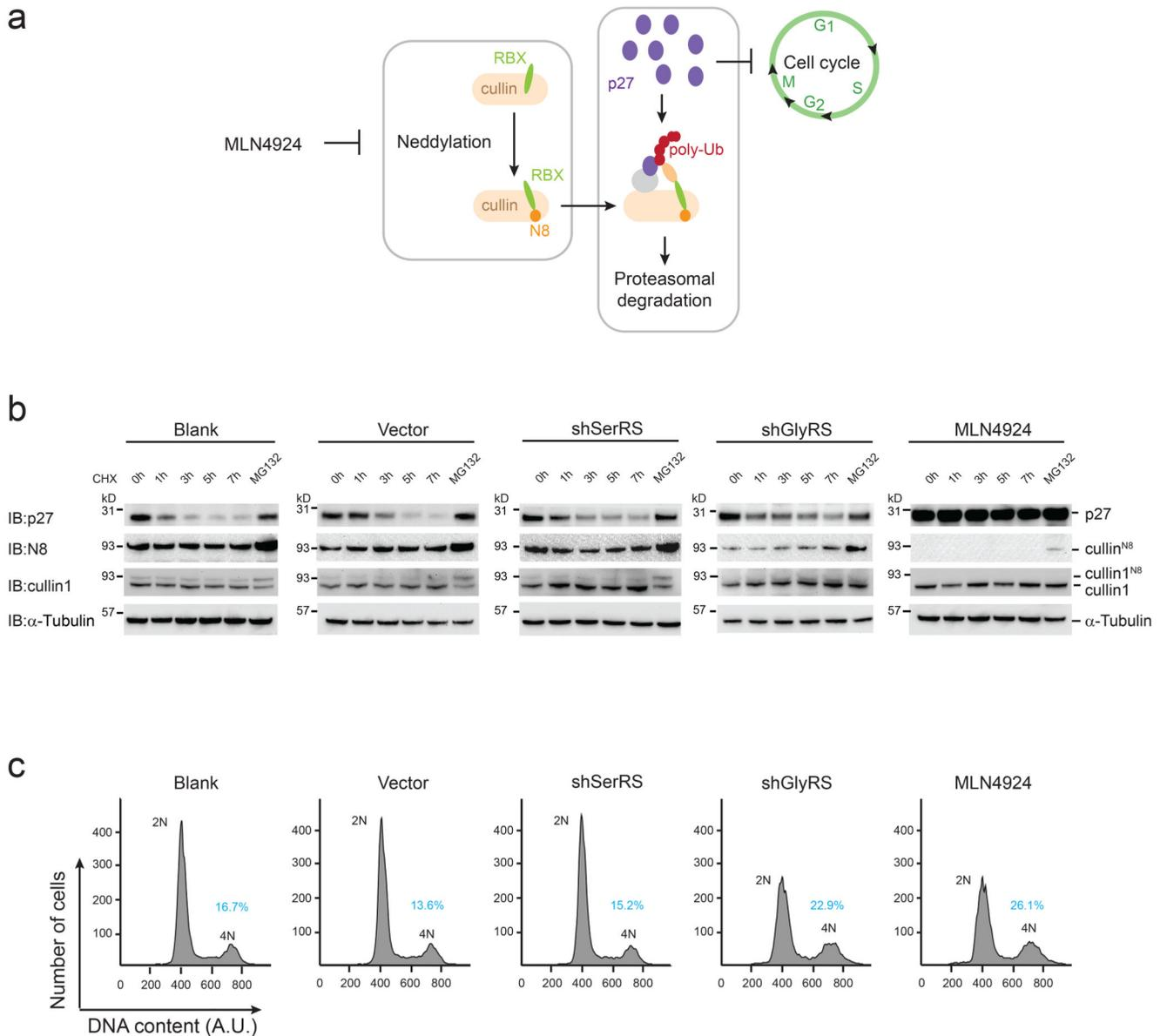


Fig. 4. GlyRS regulates cell cycle via promoting cullin neddylation

(a) A schematic figure showing how cullin neddylation controls cell cycle by activating poly-ubiquitination and proteasomal degradation of cell cycle inhibitors such as p27. (b) Western blot analysis to detect p27 and cullin neddylation in HeLa cells transfected with plasmids expressing shRNAs against GlyRS (shGlyRS) or SerRS (shSerRS) or a control vector, or treated with MLN4924 prior to cycloheximide (CHX) treatment. (c) Cell cycle analysis using HeLa cells transfected with plasmids expressing shRNAs against GlyRS (shGlyRS) or SerRS (shSerRS) or a control vector, or treated with MLN4924. DNA content was stained by propidium iodide (PI) and indicated as Arbitrary Unit (A.U.). Percentages of 4N cells are labeled.

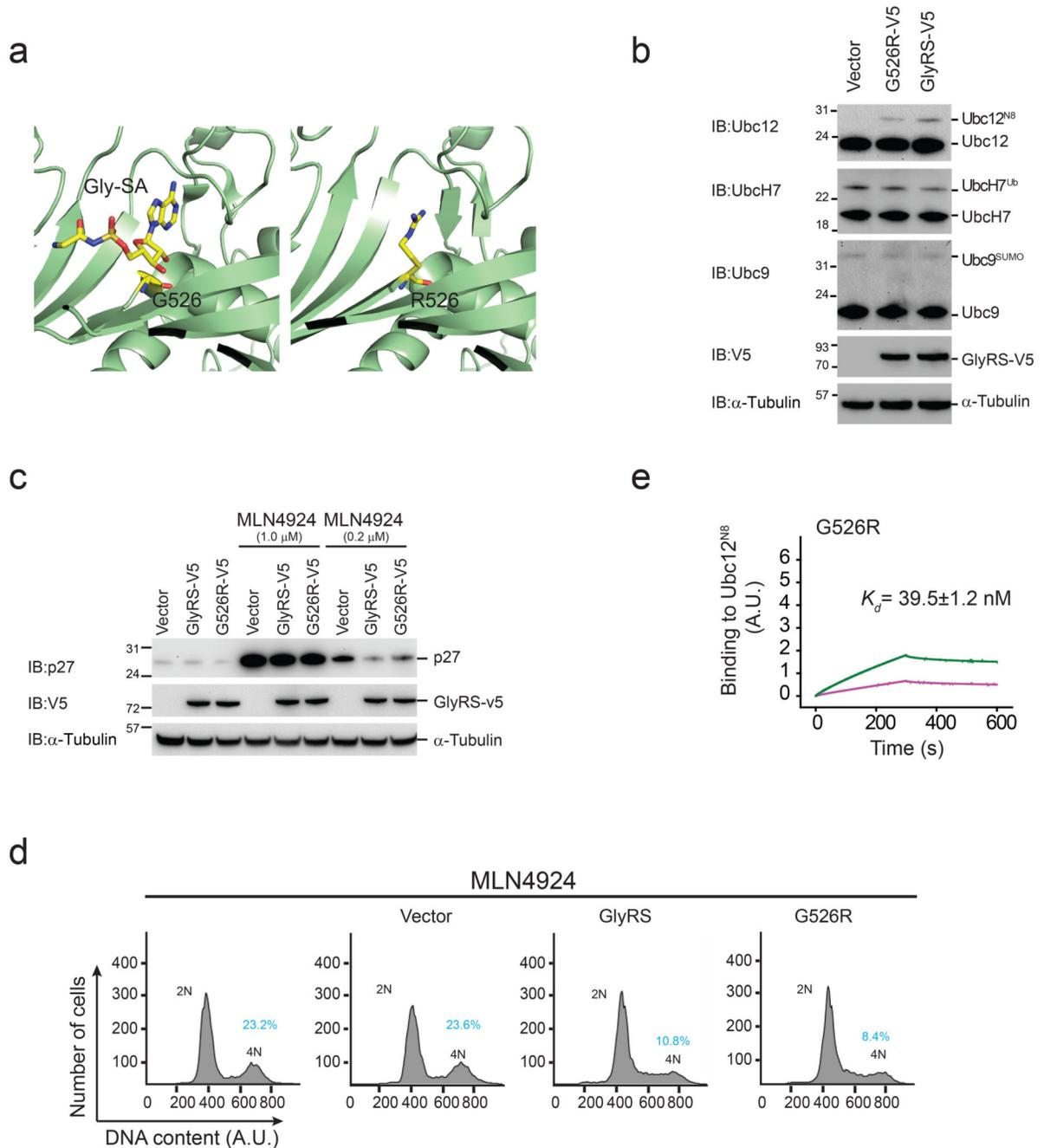


Fig. 5. Active site is involved but not essential for GlyRS role in neddylation

(a) Crystal structure of the active site of human GlyRS bound with glyceryl-sulfamoyladenine (Gly-SA) (PDB 2ZT8) and of human G526R GlyRS (PDB 2PMF). (b) Western blot analysis to compare the effect of overexpressing G526R versus WT GlyRS on E2 conjugations in HEK293 cells. (c) Western blot analysis to detect the effect of overexpressing G526R versus WT GlyRS on p27 level in HeLa cells, in the absence and presence of MLN4924. (d) Cell cycle analysis of HeLa cells overexpressing G526R or WT GlyRS and of control cells, in the presence of MLN4924. DNA content was stained by

propidium iodide (PI) and indicated as Arbitrary Unit (A.U.). Percentages of 4N cells are labeled. **(e)** Biolayer interferometry analysis to quantify G526R GlyRS (62.5-125 nM) binding to immobilized Ubc12^{N8}. N=4, error indicates S.D.

Author Manuscript

Author Manuscript

Author Manuscript

Author Manuscript

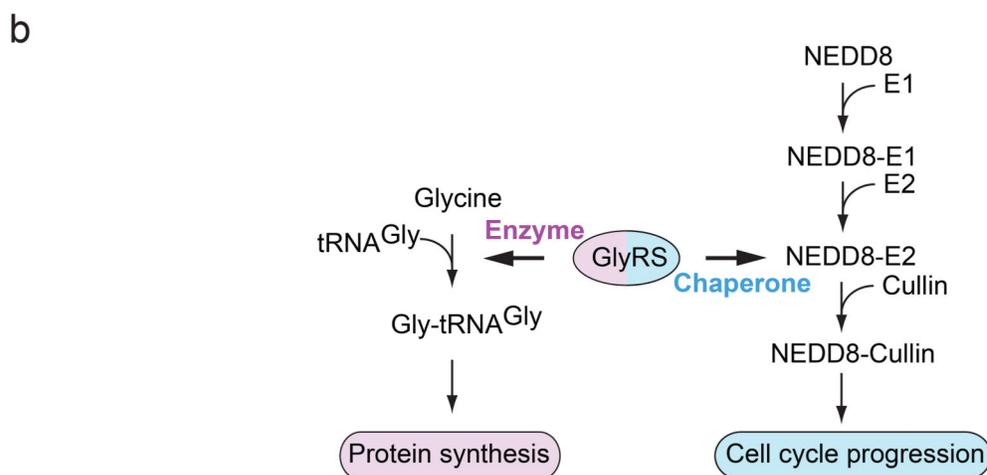
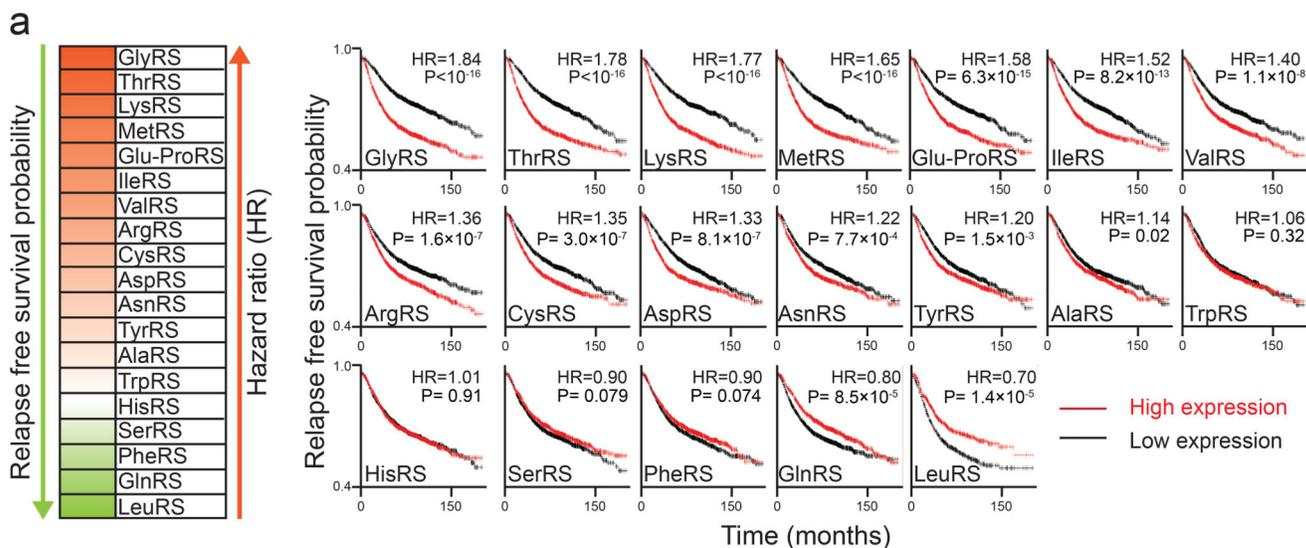


Fig. 6. Dual function of GlyRS in protein synthesis and neddylation

(a) Kaplan-meier plots and hazard ratio analysis of human tRNA synthetases in breast cancer. Patient samples were divided in two halves as “low-expression (black)” and “high-expression (red)” sets for each tRNA synthetase in the analysis. N=3557. (b) A schematic illustration to summarize the dual function of GlyRS in aminoacylation as an enzyme and in neddylation as a chaperone to support protein synthesis and cell cycle progression, respectively.